Electronic Supplementary Material (ESI) for Energy & Environmental Science

Supplementary Information

Steric hinderance-induced formation of zwitterionic carbonates from alkanolamines and CO_2: highly efficient CO_2 absorbents

Jinkyu Im, Sung Yun Hong, Youngeun Cheon, Jeesun Lee, Je Seung Lee, Hoon Sik Kim, Minserk Cheong,* and Hoseok Park**

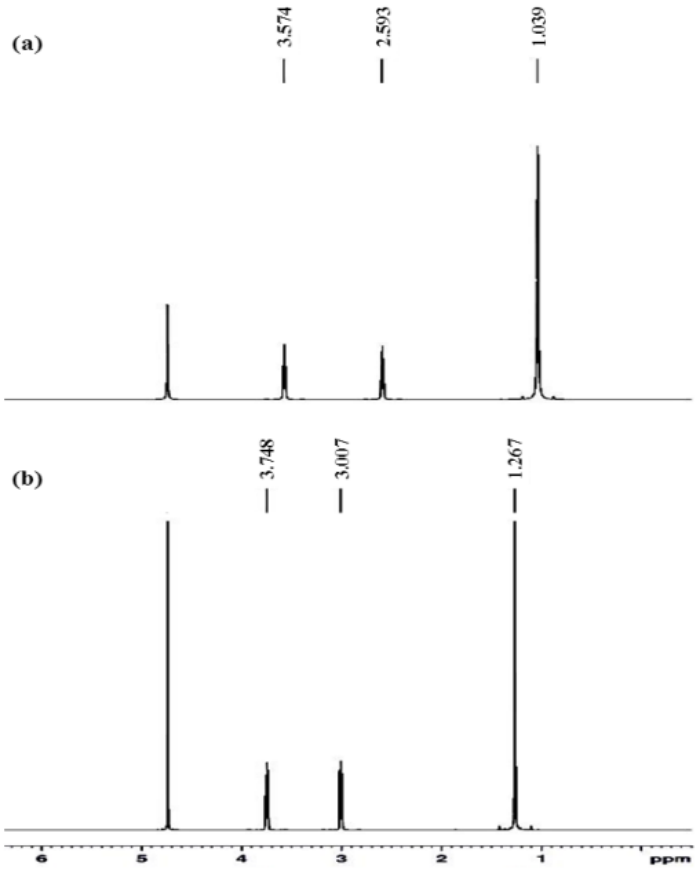

Fig. S-1 ^{1}H NMR spectra of TBA and TBAE-CO_2 in D_2O.

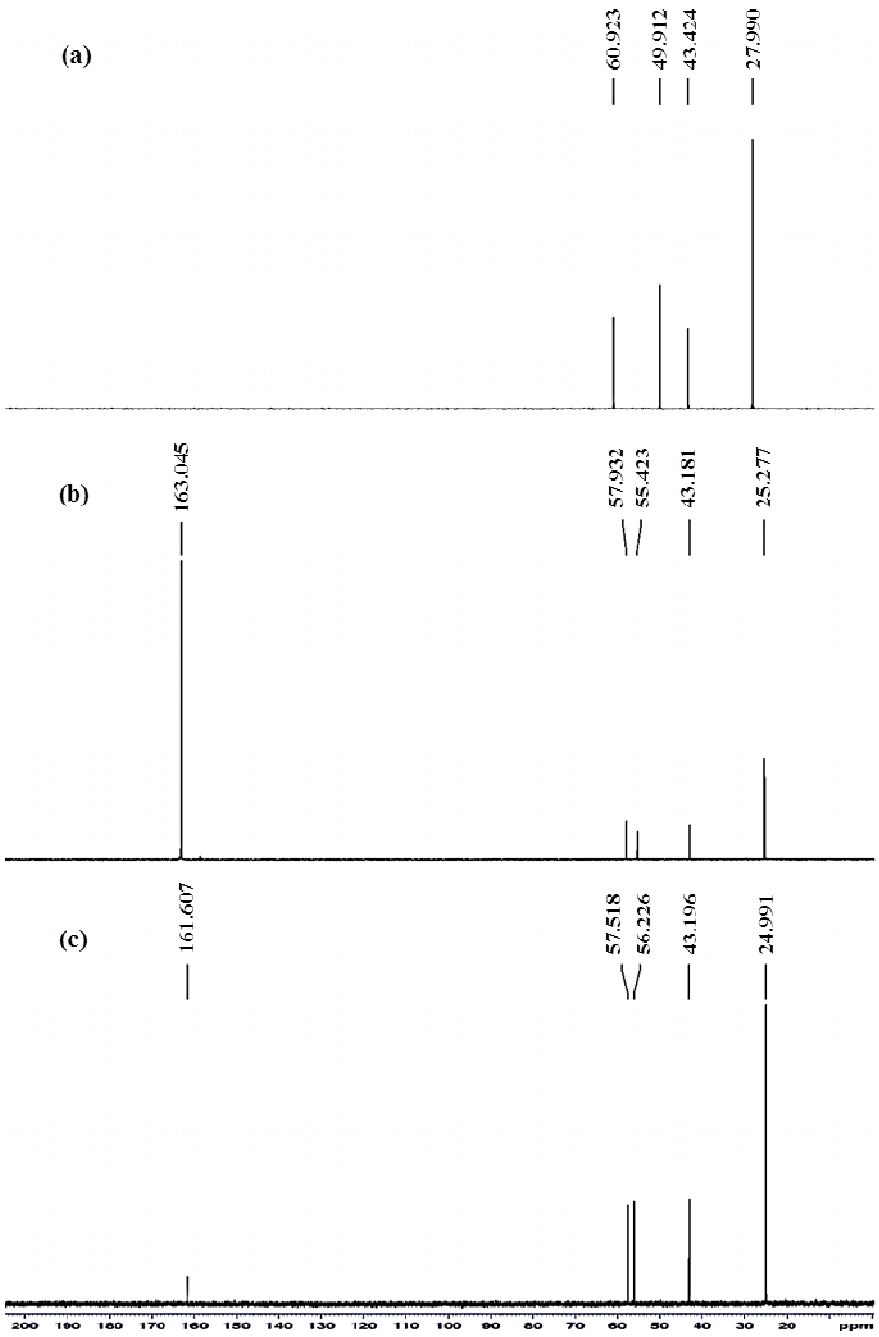

Fig. S-2 ^{13}C NMR spectra of TBA and TBA-CO_2 adducts in D_2O: (a) TBAE, (b) TBAE-$^{13}CO_2$, (c) TBAE-$^{12}CO_2$.

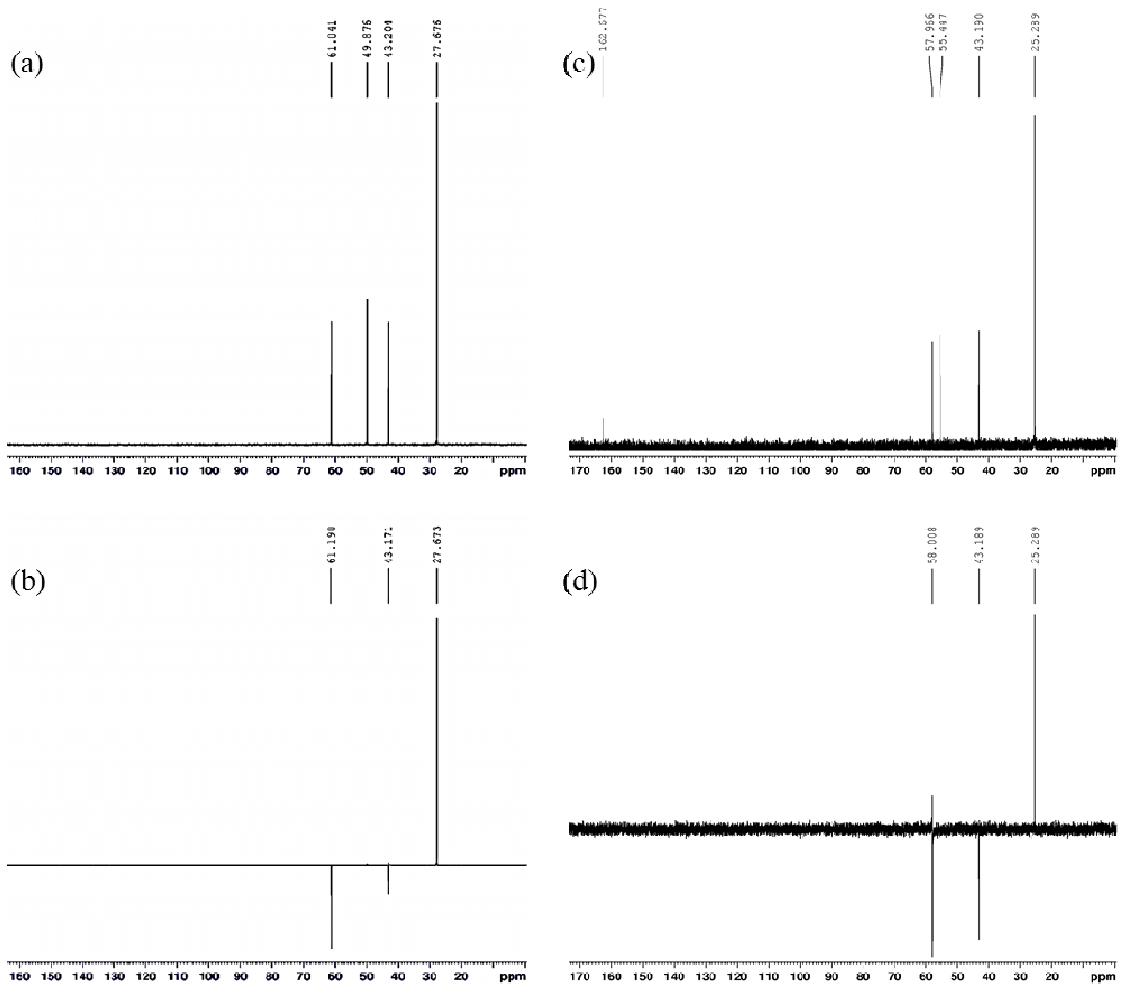

Fig. S-3 DEPT-135 spectra of TBA and TBA-CO_2 adducts in D_2O: (a) ^{13}C NMR of TBAE, (b) DEPT-135 of TBAE, (c) ^{13}C NMR of TBAE-CO_2, (b) DEPT-135 of TBAE-CO_2.

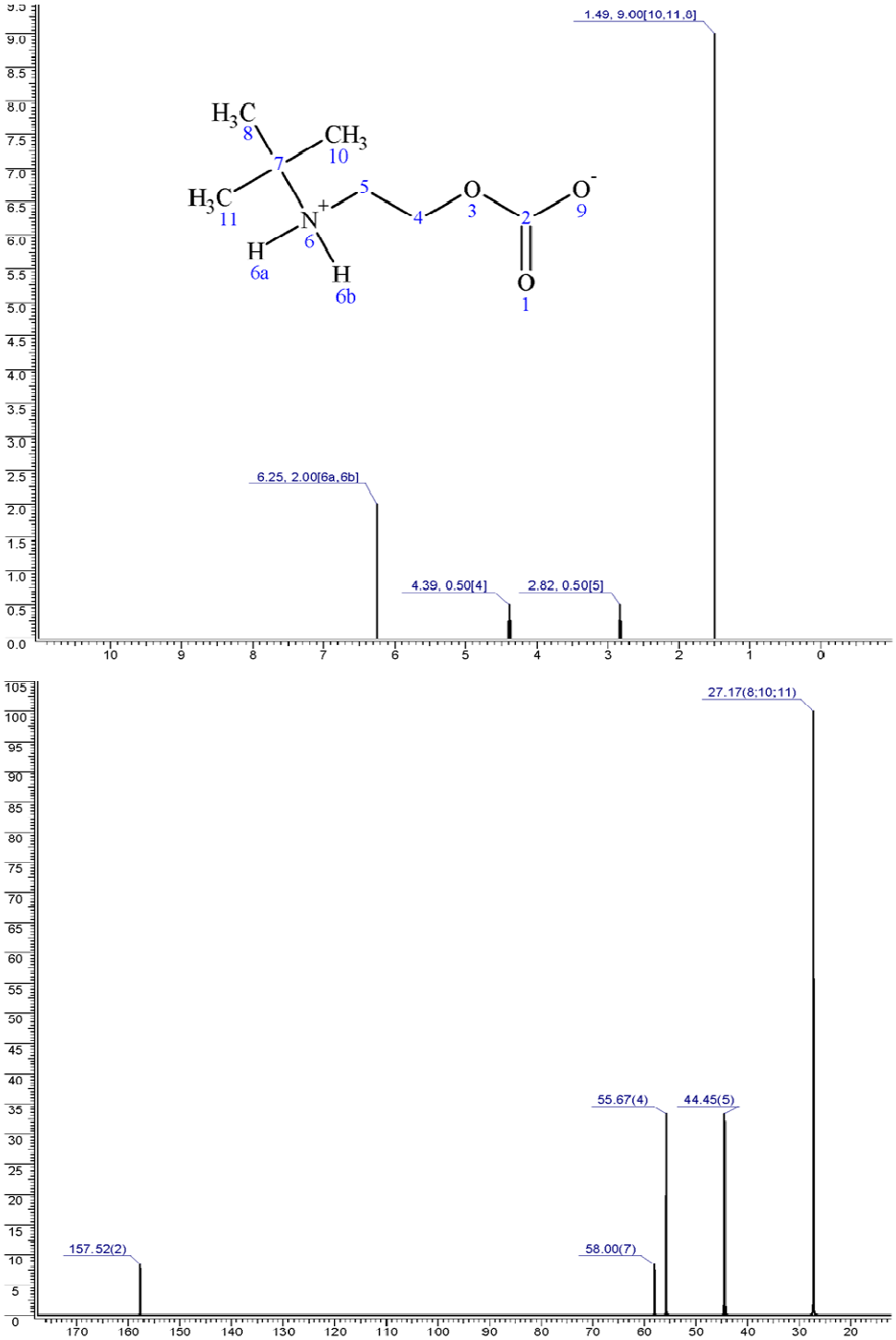

Fig. S-4 Predicted NMR spectra of t-$C_4H_9NH_2^+CH_2CH_2OCO_2^-$ using ACD/NMR DB (v.6.12) software: (top) ^{1}H NMR, (bottom) ^{13}CNMR.

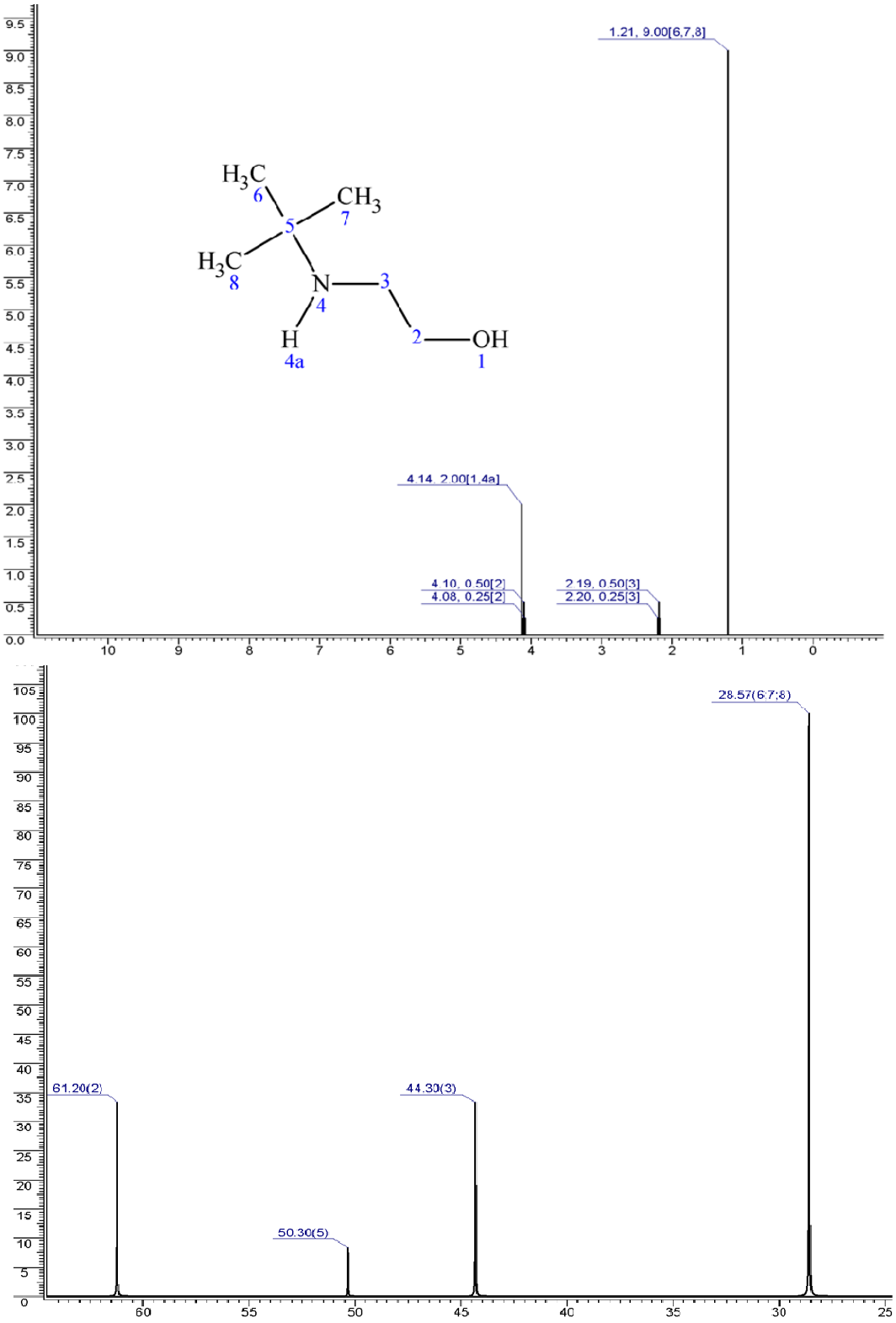

Fig. S-5 Predicted NMR spectra of TBAE using ACD/NMR DB (v.6.12) software: (top) ^{1}H NMR, (bottom) ^{13}C NMR.

Fig. S-6 A photograph of a high perssure FT-IR cell.

Fig. S-7 Schematic diagram of CO_2 absorption-desorption apparatus

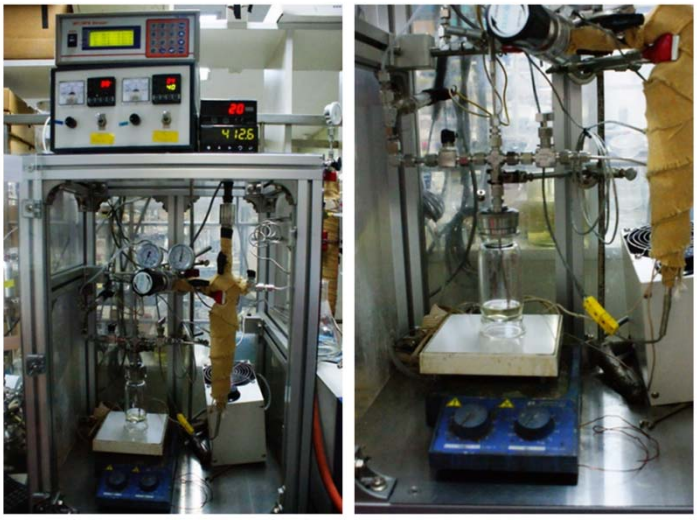

Fig. S-8 A CO_2 absorption apparatus used for the CO2 absorption capacity of TBAE solution in diethyl ether and for the synthesis of TBAE-CO_2 adduct.

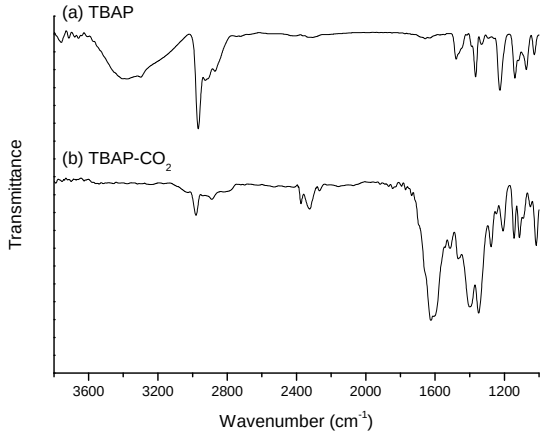

Fig. S-9 IR spectra showing the interactions of neat TBAP with CO_2.

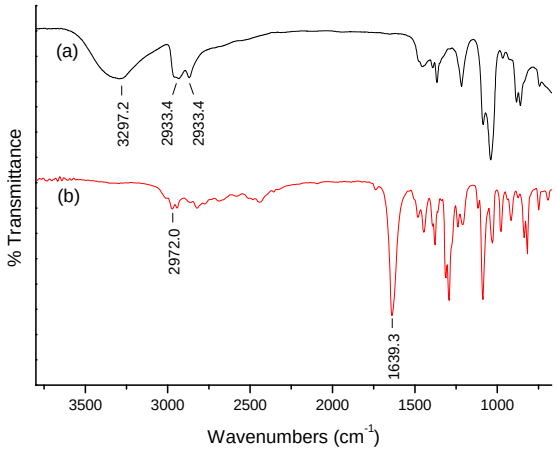

Fig. S-10 FT-IR spectrum of the neat TBAE and TBAE-CO_2 adduct isolated from the reaction of the TBAE with CO_2 in diethyl ether.

A: Carbamate pathway

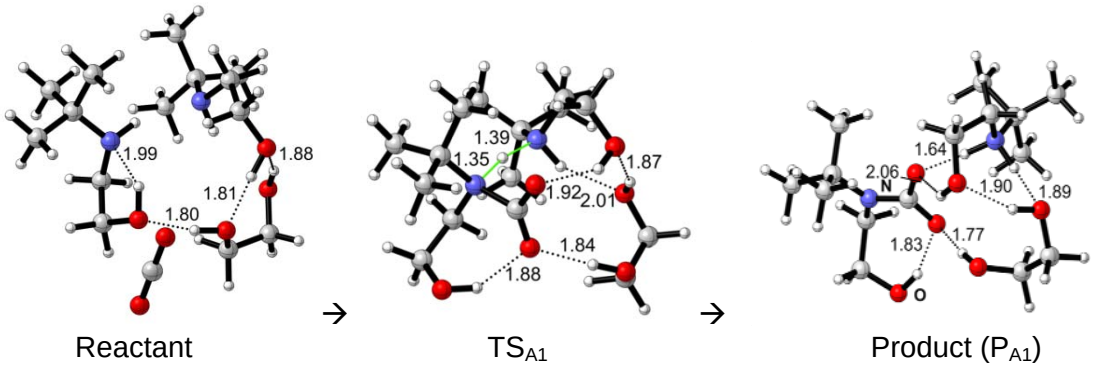

Reactant → TS_{A1} → Product (P_{A1})

B: Carbonate pathway

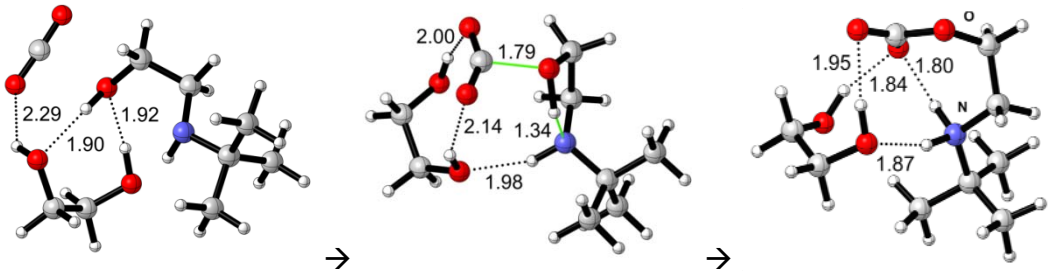

Reactant → TS_{B1} → Product (P_{B1})

Fig. S-11 Optimized structures showing the interactions of TBAE with CO_2. Pathway A: (TS_{A1}) transition state ($\Delta G^{\ddagger}_{\mathbf{TSA1}}$ = 30.1 kcal/mol), (P_{A1}) TBAE-CO_2 adduct (ΔG_{PA1} = 1.4 kcal/mol); Pathway B: (TS_{B1}) transition state ($\Delta G^{\ddagger}_{TSB1}$ = 16.4 kcal/mol), (P_{B1}) TBAE-CO_2 adduct (ΔG_{PB1} = -2.8 kcal/mol).

A: Carbamate pathway

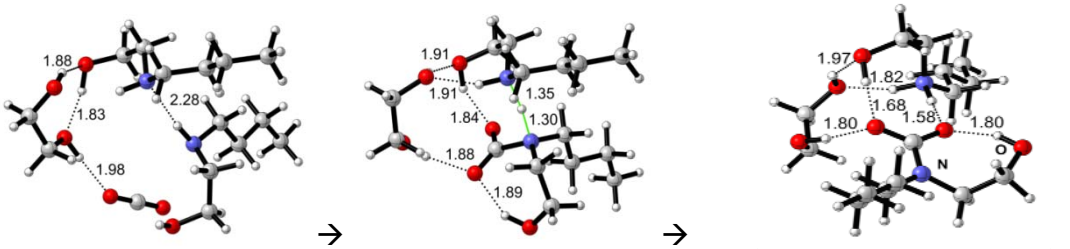

Reactant → TS_{A2} → Product (P_{A2})

B: Carbonate pathway

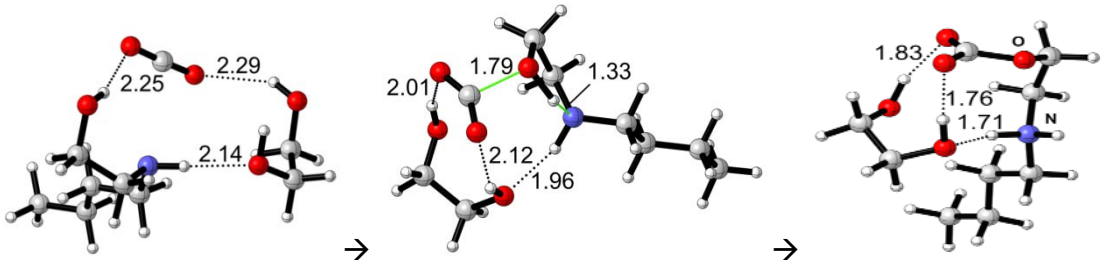

Reactant → TS_{B2} → Product (P_{B2})

Fig. S-12 Optimized structures showing the interactions of BAE with CO_2. Pathway A: (a) transition state ($\Delta G^{\ddagger}_{TSA2}$ = 3.9 kcal/mol), (b) BAE-CO_2 adduct (ΔG_{PA2} = -20 kcal/mol); Pathway B: (c) transition state ($\Delta G^{\ddagger}_{TSB2}$ = 18.7 kcal/mol), (d) BAE-CO_2 adduct (ΔG_{PB2} = 2.5 kcal/mol).

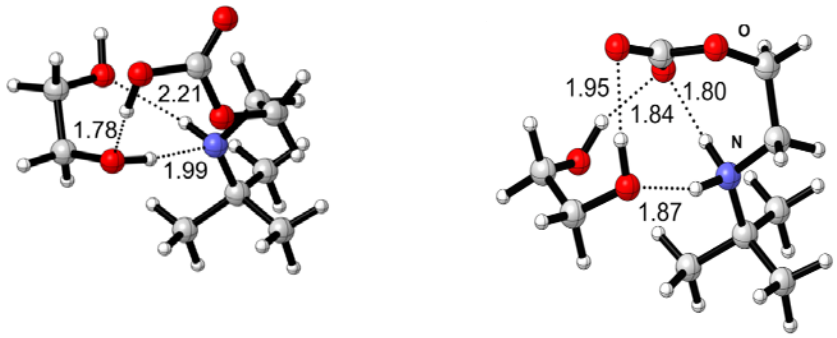

Fig. S-13 Optimized structures of the intermediate carbonic acid species (left, ΔG = +4.1 kcal/mol) and carbonate (right, ΔG = -2.8 kcal/mol) formed from the interaction of TBAE with CO_2.

A'1: Carbamate pathway for TBAE in the absence of EG

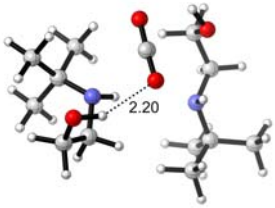

Reactant (0.0 kcal/mol)

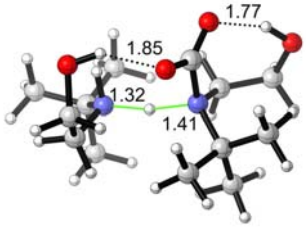

$TS_{A'1}$ (+28.5 kcal/mol)

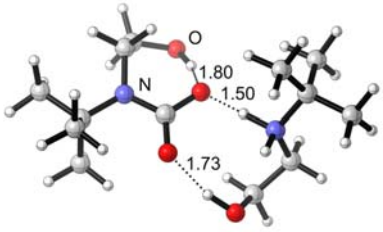

Product ($P_{A'1}$) (-5.4 kcal/mol)

B'1: Carbonate pathway for TBAE in the absence of EG

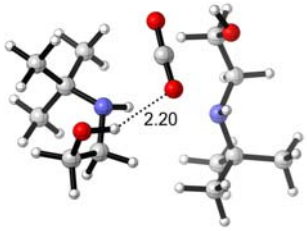

Reactant (0.0 kcal/mol)

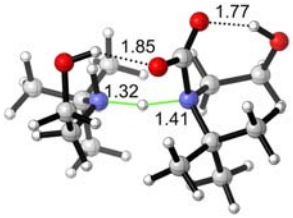

$TS_{B'1}$ (+10.7 kcal/mol)

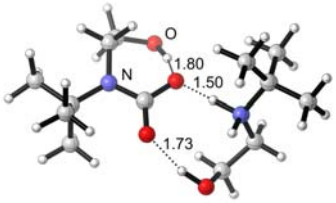

Product ($P_{B'1}$) (-0.9 kcal/mol)

A'2: Carbamate pathway for BAE in the absence of EG

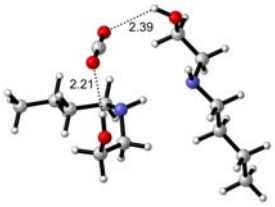

Reactant (0.0 kcal/mol)

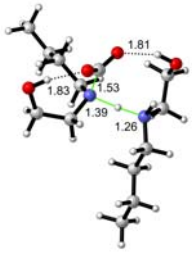

$TS_{A'2}$ (+16.7 kcal/mol)

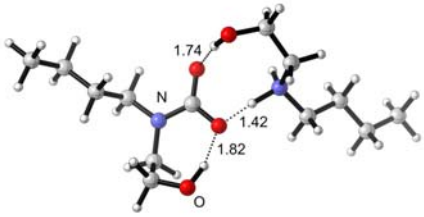

Product ($P_{A'2}$) (-4.9 kcal/mol)

B'2: Carbonate pathway for BAE in the absence of EG

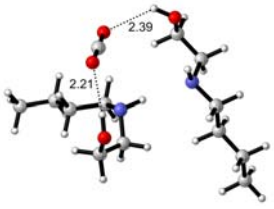

Reactant (0.0 kcal/mol)

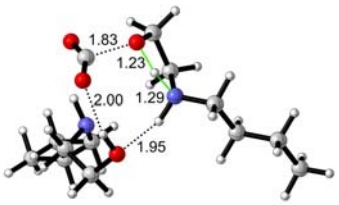

$TS_{B'2}$ (+16.3 kcal/mol)

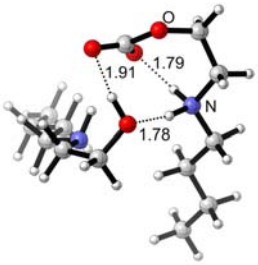

Product ($P_{B'2}$) (+5.7 kcal/mol)

Fig. S-14 Optimized structures showing the interactions of CO_2 with TBAE and BAE in the absence of EG. Pathway A': Carbamate pathway, Pathway B': Carbonate pathway.

Reference [23]

Gaussian 09 (Revision A.1), M. J. Frisch, G. W. Trucks, H. B. Schlegel, G. E. Scuseria, M. A. Robb, J. R. Cheeseman, G. Scalmani, V. Barone, B. Mennucci, G. A. Petersson, H. Nakatsuji, M. Caricato, X. Li, H. P. Hratchian, A. F. Izmaylov, J. Bloino, G. Zheng, J. L. Sonnenberg, M. Hada, M. Ehara, K. Toyota, R. Fukuda,

J. Hasegawa, M. Ishida, T. Nakajima, Y. Honda, O. Kitao, H. Nakai, T. Vreven, J. A. Montgomery, Jr., J. E. Peralta, F. Ogliaro, M. Bearpark, J. J. Heyd, E. Brothers, K. N. Kudin, V. N. Staroverov, R. Kobayashi, J. Normand, K. Raghavachari, A. Rendell, J. C. Burant, S. S. Iyengar, J. Tomasi, M. Cossi, N. Rega, J. M. Millam, M. Klene, J. E. Knox, J. B. Cross, V. Bakken, C. Adamo, J. Jaramillo, R. Gomperts, R. E. Stratmann, O. Yazyev, A. J. Austin, R. Cammi, C. Pomelli, J. W. Ochterski, R. L. Martin, K. Morokuma, V. G. Zakrzewski, G. A. Voth, P. Salvador, J. J. Dannenberg, S. Dapprich, A. D. Daniels, O. Farkas, J. B. Foresman, J. V. Ortiz, J. Cioslowski, and D. J. Fox, Gaussian, Inc., Wallingford, CT, USA, 2009.